

## RESEARCH NOTE

# Solid Electrolytes as Active Catalyst Supports: Electrochemical Modification of Benzene Hydrogenation Activity on Pt/ $\beta''$ (Na)Al<sub>2</sub>O<sub>3</sub>

C. A. Cavalca<sup>1</sup> and G. L. Haller<sup>2</sup>

*Department of Chemical Engineering, Yale University, New Haven, Connecticut 06520*

Received July 31, 1995; revised February 9, 1998; accepted February 26, 1998

The influence of Na on benzene hydrogenation over Pt has been investigated. The amount of Na interacting with the Pt catalyst was reversibly changed by electrochemically pumping the Na from  $\beta''$ -Al<sub>2</sub>O<sub>3</sub>, a solid electrolyte which was both the Pt support and the source of the Na. The kinetics of the reaction are affected in a way that indicates an electronic effect of Na on benzene adsorption. The reaction can be completely inhibited at apparently low coverages of Na relative to the total surface area measured by oxygen chemisorption which may imply that only a small fraction of this surface is active for benzene hydrogenation on Pt/ $\beta''$ -Al<sub>2</sub>O<sub>3</sub>. © 1998 Academic Press

### INTRODUCTION

The use of solid electrolytes (fast ion conductors) as active catalyst supports has been associated with the concept of electrochemical promotion in heterogeneous catalysis (1). The concept of non-Faradaic catalysis is based upon the electronic and, perhaps also geometric, reversible changes that take place on a catalyst surface. The surface is perturbed by electrochemically controlled spillover of catalytic promoter/poison species moved to or from the solid electrolyte, which acts as an active catalyst-support under pumping (potentiostatic/galvanostatic bias) conditions. This electrochemical promotion of heterogeneous catalysts is known as the NEMCA effect (non-Faradaic electrochemical modification of catalytic activity) (2). It may be considered as a very effective way to reversibly tune the dosage of catalyst promoter (or poison, depending upon the system) that one can introduce on a catalyst surface electrochemically.

Previous work on the subject mainly concerned oxidation reactions over a wide variety of metal catalysts. The solid electrolytes used have been mainly of two kinds: yttria-

stabilized-zirconia (an oxide conductor) and  $\beta''$ -Al<sub>2</sub>O<sub>3</sub>, a Na<sup>+</sup> conductor. A review of the state of the art of electrochemical promotion has been presented by Vayenas (3).

We believe this work to be the first to demonstrate electrochemical modifications of catalytic activity for an hydrogenation reaction. The electrolyte used was  $\beta''$ -Al<sub>2</sub>O<sub>3</sub>, a Na<sup>+</sup> conductor, and the catalytic metal was Pt. Thus the  $\beta''$ -Al<sub>2</sub>O<sub>3</sub> may be said to be an active support in the sense that Na<sup>+</sup> from the support can be transported to and from the Pt and alter its activity. However, this is a simpler case than when O<sup>2-</sup> conductors are used for oxidation reactions where the O<sup>2-</sup> may both modify the activity of the catalytic electrode and become a reactant.

### EXPERIMENTAL

The electrocatalytic reactor used was of the CFSTR-single pellet type (4) (Fig. 1a) in which all the electrodes (catalyst/working + additional electrodes) are exposed to the reacting mixture. The cell configuration is presented on Fig. 1b. It consists of the solid electrolyte (fast-ion-conductor oxide, which under externally induced bias conditions acts as a source or sink of charge-carrier ionic species), with a working-electrode (the catalyst, Pt in our case) and a counter-electrode (Ag). A silver reference-electrode is also added in order to monitor overvoltages.

The bare electrolyte cylinder (Plyceram) was first baked in air at 800°C in order to eliminate adsorbed water and sublimate surface carbonates before the electrodes were applied. The porous platinum catalysts used through all the experiments were prepared by applying thin coatings of a Pt organometallic (Pt resinate, Engelhard A-1121) on the solid electrolyte followed by drying at 400°C and calcination at 830°C. It was found that two coats of Pt ink, followed by their respective drying-calcination procedures, sufficed to produce an electrically conductive and uniform deposition. An electrode prepared this way typically presented a Pt

<sup>1</sup> Present address: W. L. Gore & Asso. P.O. Box 1100, Elkton, MD 21922.

<sup>2</sup> Corresponding author. E-mail: gary.haller@yale.edu.

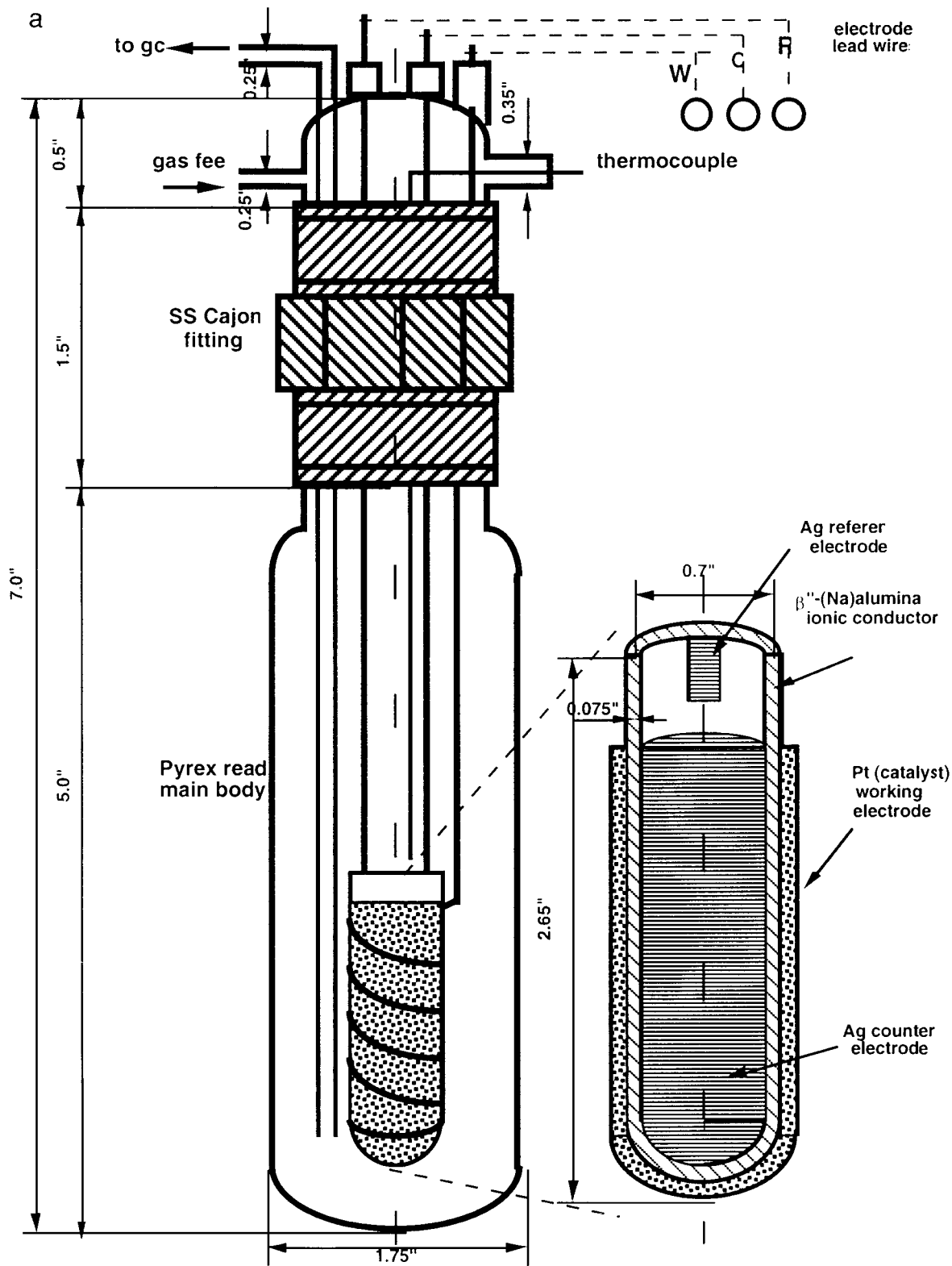


FIG. 1. (a) CFSTR electrocatalytic single pellet reactor. (b)  $C_6H_6$ ,  $H_2$ , Pt/ $\beta''$ -(Na)Al $_2$ O $_3$ /Ag single pellet cell configuration.

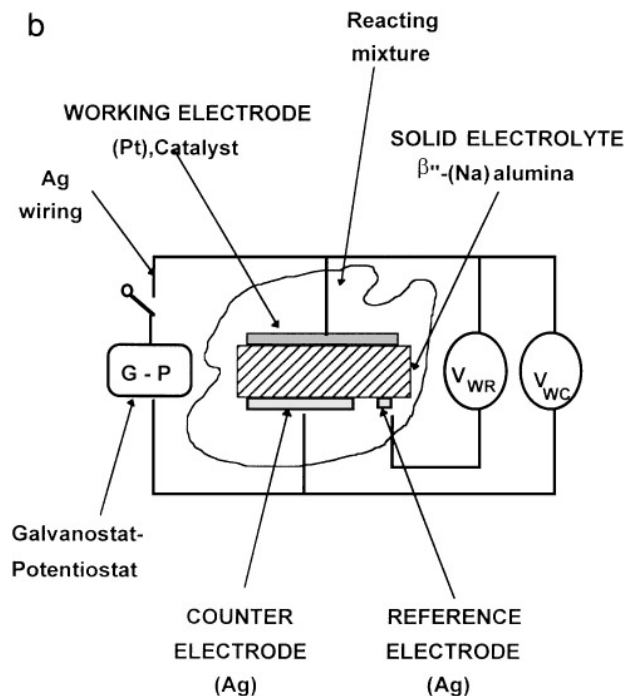


FIG. 1—Continued

loading of  $26 \text{ mg/cm}^2$  with a catalyst film thickness of about  $15 \mu\text{m}$ . The true surface area of the Pt catalyst was  $3540 \text{ cm}^2$ , as measured using the isothermal titration technique (2). In brief, the surface is saturated with  $\text{O}_2$  at ambient temperature and the chemisorbed oxygen reacted with  $\text{C}_2\text{H}_4$  and the amount of  $\text{CO}_2$  produced is measured. The Ag counter and reference electrodes were obtained from a commercial suspension of metallic silver in butyl acetate (GC electronics), followed by drying plus calcination at  $300^\circ\text{C}$ . The counter electrode (with a geometrical surface area approximately equal to the one of the working electrode) was placed on the opposite side of the solid electrolyte, symmetrical to the working electrode. The reference electrode presented a geometric surface area one order of magnitude smaller than the working (catalyst) electrode.

The exit of the reactor was sampled and analyzed by on-line gas chromatography. All gases were UHP grade. The benzene (here carried by He from a bubble saturator with the saturation pressure controlled via condenser) was reagent grade. Before each reaction, the Pt catalyst was cleaned *in situ* by cycling between oxidation and reduction in pure  $\text{O}_2$  and  $\text{H}_2$  at  $200^\circ\text{C}$ .

The potential was measured, applied, and controlled using an EG&G Versastat potentiostat/galvanostat. The analog output of the potentiostat was sampled by a SMAD (a special Macintosh-compatible interface, Morgan Kennedy Research, used to process and digitize the signal) interface to facilitate data handling and analysis.

Coulometry, the integration of a current-time wave produced by the cell as a response to a potential step, is a direct

method of measuring  $\text{Na}^+$  transport (coverage). The total number of g-atoms of  $\text{Na}^+$  ( $n_{\text{Na}}$ ) transferred during the evolution of the current-time wave is:

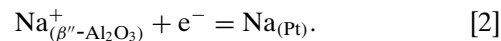
$$n_{\text{Na}} = (1/F) \int_{t=0}^{\infty} I_{\text{WC}}(t) dt, \quad [1]$$

where  $F$  is the Faraday constant and  $I_{\text{WC}}$  is the measured ionic current flowing between the working and counter electrodes. This integration was typically made for each potentiostatic jump of a series of several positive jumps in potential, a regeneration, i.e., potentiostatic setting equal to the initial potential and several negative overpotential applications. Thus, having measured the total number of g-atoms of  $\text{Na}^+$  transferred at a given  $V_{\text{WR}}$  and the true surface area of the catalyst obtained by surface titration, the coverage as a function of potential can be calculated.

## RESULTS AND DISCUSSION

Figure 2 shows the steady-state effect of applied catalyst potential  $V_{\text{WR}}$  (potential of the Pt catalyst referred to the Ag reference electrode) on the activity to cyclohexane production. The data shows that by potentiostatically biasing the cell with voltages more positive than the open circuit emf (marked on the plot as  $V_{\text{WR}}^0$ ) we can obtain an improvement in activity up to two times the open circuit value (represented by the enhancement ratio  $\rho$ , defined as the ratio of the rate with applied potential to the open circuit rate). Furthermore, making the potential of the catalyst more negative than its equilibrium emf causes a decrease in activity, reducing it to almost zero for  $\Delta V_{\text{WR}} = -200 \text{ mV}$  ( $\Delta V_{\text{WR}}$  represents the deviation of potential from the open circuit emf,  $V_{\text{WR}}^0$  is due to externally imposed bias and is given by the difference  $V_{\text{WR}} - V_{\text{WR}}^0$ ).

The electrocatalysis taking place at the TPB (three phase boundary), i.e., at the perimeter of contact between Pt, gas, and solid electrolyte, indicates that positive overpotentials  $\Delta V_{\text{WR}}$  induce Na removal from the Pt surface following the redox



Thus, Na stripping from the Pt surface causes a beneficial effect on the activity and the opposite is true for negative potentials, i.e., Na doping onto the Pt surface causes a decrease in activity. This demonstrates that in the Pt electrode preparation (calcination at  $830^\circ\text{C}$ ) some  $\text{Na}^+$  ions from the  $\beta''\text{-Al}_2\text{O}_3$  electrolyte support have interacted with the Pt. The electrocatalytic redox [2] is the dominant charge transfer reaction, as previous Pt/ $\beta''\text{-Al}_2\text{O}_3$  NEMCA studies have also shown (3, 7, 8). In a recent paper, Lambert and coworkers (9) have shown that Na adsorbed on the Pt surface electrode certainly exists and has similar dipole moment as adsorbed Na introduced from the gas phase. In addition, solid electrolyte cyclic voltammetry experiments on

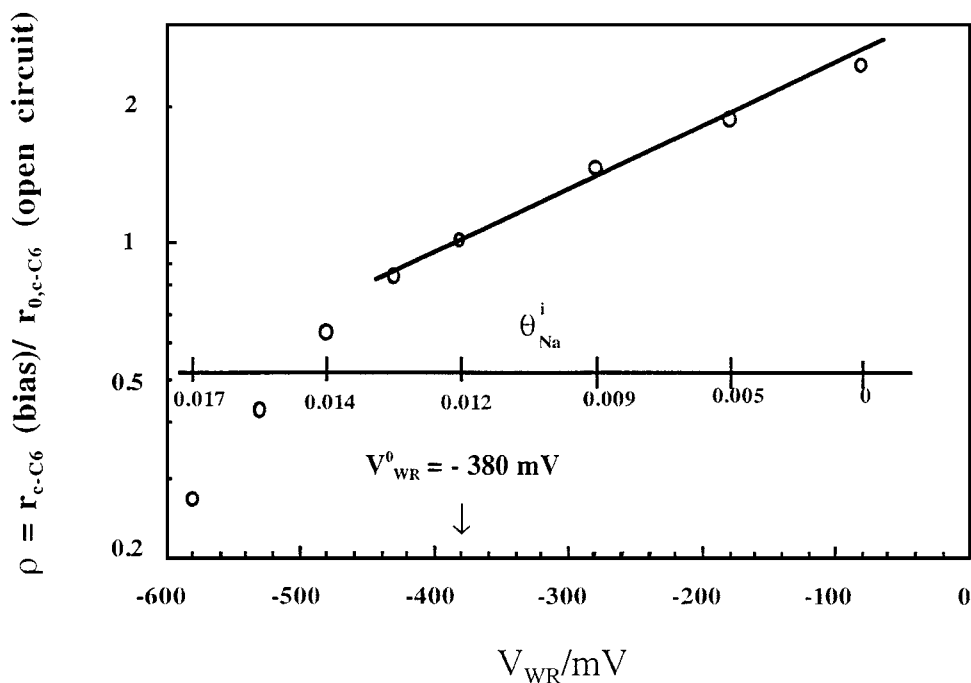


FIG. 2. Activity-polarization-curve equivalent diagram. Open circuit potential,  $V_{\text{WR}}^0 = -380$  mV,  $T_{\text{reaction}} = 130^\circ\text{C}$ ,  $p_{\text{H}_2} = 33.35$  kPa,  $p_{\text{C}_6\text{H}_6} = 2.02$  kPa, total pressure 1 atm,  $\phi_{(\text{reactor space time})} = 0.17$  min $^{-1}$ ,  $F_{\text{total}} = 81$  cm $^3$  (STP)/min.

the single-pellet Pt/ $\beta''$ -Al $_2$ O $_3$ /Ag system (5) have shown the presence of anodic peaks (i.e.,  $\text{Na}_{(\text{Pt})} \rightarrow \text{Na}_{(\beta''\text{-Al}_2\text{O}_3)}^+ + e^-$ ) and cathodic peaks (i.e.,  $\text{Na}_{(\beta''\text{-Al}_2\text{O}_3)}^+ + e^- \rightarrow \text{Na}_{(\text{Pt})}$ ) at temperatures and gaseous atmospheres equivalent to reaction conditions.

It is important to emphasize that electrochemically induced and controlled backspillover of Na (which is proposed to be the cause of NEMCA (2, 3, 5, 8) starts from the three-phase boundary (TPB) and takes place over the entire gas-exposed (catalytic) electrode surface. The three phase boundary, i.e., the perimeter of contact between the solid electrolyte, metal catalyst and gas phase, is the electrocatalytically active site, where the charge transfer reactions take place. NEMCA involves changes of catalytic activity onto the entire gas-exposed (catalytically active) metal surface and is not limited to the TPB.

By further examining the activity-polarization curve (Fig. 2) we also observe that, in the range of potential between 0 and  $-400$  mV, the rate varies exponentially with the catalyst potential.

$$\ln \rho = \alpha F(V_{\text{WR}} - V_{\text{WR}}^*)/RT. \quad [3]$$

Here  $V_{\text{WR}}^*$  and  $\alpha$  are catalyst/reaction/electrode-electrolyte specific constants and  $F$  is the Faraday constant. This kind of behavior is consistent with previous work (2, 3) that suggests that over wide ranges of catalyst surface work function, catalytic rates depend exponentially on  $e\Phi$  in concordance with Vayenas' Kelvin probe measurements (2, 3)

suggesting the relation  $e\Delta V_{\text{WR}} = \Delta e\Phi$ . Although the exact physical meaning of  $\alpha$  and  $V_{\text{WR}}^*$  is still unclear (3), the NEMCA coefficient  $\alpha$  is an indication of the electrophobic character of the reaction: the  $\alpha$  parameter becomes positive for electrophobic reactions and negative for electrophilic ones and typically takes values between  $-1$  and  $1$  (3, 13). Furthermore, the parameter  $V_{\text{WR}}^*$  can be understood as a threshold cell potential (or threshold overpotential, if  $\eta_{\text{WR}}$  is used instead of  $V_{\text{WR}}$ ) (3).<sup>1</sup>

Sodium coverages were calculated by integration of the potentiostatically induced ionic-current waves (see Ref. (5)

<sup>1</sup> Further rationalization of the experimental relationship [3] and the NEMCA coefficients  $\alpha$  and  $V_{\text{WR}}^*$  can be attained if we consider Eq. [3] as a semi-empirical relation that can be written, consistent with the analogy presented by the high-field form of the Butler-Volmer equation (Tafel approximation),  $\ln(I/I_0) = \alpha_0 F(V_{\text{WR}} - V_{\text{WR}}^0)/RT$  for anodic operation and  $\ln(-I/I_0) = -\alpha_c F(V_{\text{WR}} - V_{\text{WR}}^0)/RT$  for cathodic operation. This equation governs the electrocatalytic charge-transfer reactions that take place at the TPB at high (ca  $|\eta| > 100$  mV) overpotentials. The coefficients  $\alpha_a$  and  $\alpha_c$  are the anodic and cathodic transfer coefficients, respectively. They are a function of the number of electrons transferred and the so-called symmetry factor  $\beta$ , which is the fraction of the potential across the double layer promoting the cathodic reaction and represents a measure of the symmetry of the electrocatalytic (charge transfer) activation barrier (14). Like the  $\alpha$  parameter in Eq. [3], the magnitude of  $\alpha_a$  and  $\alpha_c$  is usually bounded between 0 and 1. The term  $V_{\text{WR}}^0$  represents the thermodynamic equilibrium open circuit potential (emf). The similarity between the Tafel equations, which govern the rates of *electrocatalytic* reactions both in aqueous and solid-state electrochemistry and Eq. [3], which models the rate of *catalytic* reaction versus cell potential, underlines a fundamental similarity between electrochemistry and heterogeneous catalysis (3).

for details). Each potential jump is associated with a Na migration to or from the solid electrolyte through the redox reaction of Eq. [2]. The Pt surface is Na-free for  $\Delta V_{WR} = 300$  mV. The integration shows that sodium coverages of about 0.02 are needed to decrease the activity by almost a factor of 5 over the open circuit value, compared with the coverage of 0.012 observed on the fresh catalyst under open circuit. It should be noted that the latter coverage is the, presumably, equilibrium coverage at the calcination temperature. Note that this thermally induced coverage by  $\text{Na}^+$  can be reversed electrochemically, i.e., by the reverse of [2]. This implies that the thermally driven migration of  $\text{Na}^+$  must involve a reaction like [2] also. Unfortunately, we cannot describe this reaction in detail nor are we able to determine the oxidation half-reaction that accompanies it. However, the low Na coverages measured in the course of this experiment are consistent with previous work in the Pt/ $\beta''$ - $\text{Al}_2\text{O}_3$  system (7, 8) which have shown that Na coverages of the order of 0.03 suffice to decrease the work function by  $\approx 1$  eV and induce a dramatic change in catalytic activity.

Figure 3 shows the whole range of benzene hydrogenation kinetics as a function of pressure and the effect of potential application. The open circuit ( $I_{WC} = 0$ ) condition, indicates null current between the working and counter electrodes. The shape of the curve clearly reflects the presence of two different kinetic regimes, depending upon the partial pressure of benzene. At moderately low partial pressures of hydrocarbon the reaction is first order on benzene,

i.e., the rate scales linearly with the partial pressure (the slope of this linear part is proportional to the adsorption coefficient); nevertheless as the partial pressure of hydrocarbon increases the rate becomes less sensitive to this parameter, reaching a point where, at high benzene partial pressures, the rate is independent of the benzene pressure, i.e., it has a zero-order dependence. This behavior, commonly found in catalytic systems, is referred to as saturation kinetics (6). The observed zero-order dependence on the rate agrees with previous work on supported Pt catalysts (10, 11) under similar reaction conditions.

The experimentally observed kinetics can be satisfactorily described by a mechanism in which benzene and hydrogen adsorb reversibly onto the Pt surface, followed by an irreversible Langmuir–Hinshelwood (L-H) surface reaction step between chemisorbed hydrogen and benzene. This model assumes dissociative, noncompetitive  $\text{H}_2$  adsorption on sites different from those adsorbing benzene. The adsorption steps are taken as equilibrated, with the L-H encounter (addition of the first H atom) as the slow (rds) step of the elementary sequence:

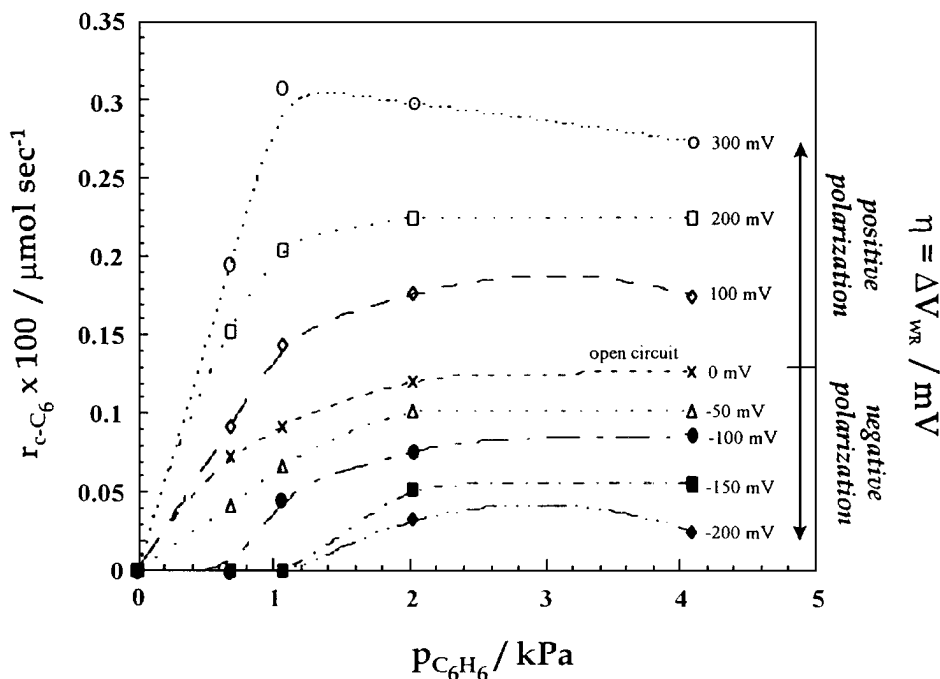
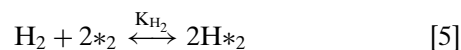
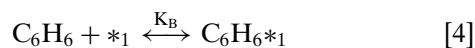


FIG. 3. Benzene hydrogenation activity mapping: Effect of benzene partial pressure and applied potential. The curves are not fits to the data but are simply drawn through the data points to clarify the qualitative behavior. Open circuit potential,  $V_{WR}^0 = -380$  mV,  $T_{\text{reaction}} = 130^\circ\text{C}$ ,  $p_{\text{H}_2} = 33.35$  kPa, total pressure 1 atm,  $\phi_{(\text{reactor space time})} = 0.17 \text{ min}^{-1}$ ,  $F_{\text{total}} = 81 \text{ cm}^3 \text{ (STP)/min}$ .

We can then write the rate expression from the rds (Eq. [6]) as

$$r = k_{\text{LH}}\theta_{\text{H}}\theta_{\text{B}} \quad [7]$$

and the adsorption elementary steps represented by a Langmuir-type isotherm, giving the classical expressions:

$$\theta_{\text{B}} = \frac{K_{\text{B}}P_{\text{B}}}{1 + K_{\text{B}}P_{\text{B}}} \quad [8]$$

and

$$\theta_{\text{H}} = \frac{(K_{\text{H}})^{1/2}P_{\text{H}_2}^{1/2}}{1 + (K_{\text{H}})^{1/2}P_{\text{H}_2}^{1/2}}. \quad [9]$$

Then, the global rate expression becomes

$$r = k_{\text{LH}} \left( \frac{(K_{\text{H}})^{1/2}P_{\text{H}_2}^{1/2}}{1 + (K_{\text{H}})^{1/2}P_{\text{H}_2}^{1/2}} \right) \left( \frac{K_{\text{B}}P_{\text{B}}}{1 + K_{\text{B}}P_{\text{B}}} \right). \quad [10]$$

The evaluation of the effect of the partial pressure of benzene on the rate was made keeping a constant partial pressure of hydrogen (as well as a constant reactor space-time); so we can assume that during the experiment the coverage of hydrogen remained approximately constant. Then we can simplify Eq. [10], setting the product  $k_{\text{LH}}\theta_{\text{H}}$  to  $k(\text{H}_2)$ . We can then rewrite Eq. [10] as

$$r = k(\text{H}_2) \left( \frac{K_{\text{B}}P_{\text{B}}}{1 + K_{\text{B}}P_{\text{B}}} \right). \quad [11]$$

If  $P_{\text{B}}$  is large enough such that  $1 + K_{\text{B}}P_{\text{B}} \approx K_{\text{B}}P_{\text{B}}$ , then Eq. [11] becomes

$$r = k(\text{H}_2). \quad [12]$$

The above rate expression is zero order in benzene and represents the saturation regime. If, on the other hand,  $P_{\text{B}}$  is small, such that  $1 + K_{\text{B}}P_{\text{B}} \approx 1$ , then Eq. [11] becomes first-order dependent in benzene partial pressure, with the rate slope proportional to  $K_{\text{B}}$ :

$$r = k(\text{H}_2)K_{\text{B}}P_{\text{B}}. \quad [13]$$

It is worth noting that our model mostly agrees with the work of Vannice *et al.*, comprising reaction models for metal surfaces on the hydrogenation of aromatic hydrocarbons over supported Pt catalysts (12). The study showed that only one model could successfully fit the benzene hydrogenation data at all temperatures. The model assumed non-competitive equilibrated  $\text{H}_2$ /benzene adsorption, addition of the first H atom as the rds, and the inclusion of concurrent hydrogenation reactions involving the aromatic reactant molecule to produce H-deficient species on the metal surface.

Examining the above data in Fig. 3, one immediately observes that the slope of the kinetic profiles in the first-

order region shifts to more positive values as the potential becomes more positive than the correspondent emf, i.e.,  $\Delta V_{\text{WR}} > 0$ . The opposite occurs as the catalyst is made more negative than  $V_{\text{WR}}^{\circ}$ . This shift is indicative of a perturbation of the benzene adsorption coefficient. As we polarize Pt positively, we increase the catalyst surface work function by  $e\Delta V_{\text{WR}} = \Delta e\Phi$  (3), favoring the adsorption of electron-donor species, like benzene. The Pt-benzene bond becomes stronger and the reaction probability increases. The opposite occurs as  $\Delta V_{\text{WR}} < 0$ , the Pt surface work function decreases, decreasing the donation of electrons from the benzene  $\pi$  orbitals, thus weakening the Pt-benzene bond.

Another interesting result which emerges from this plot is that the adsorption of hydrogen may be affected also. This can be observed from the saturation (horizontal) portion of the kinetics. If adsorbed hydrogen (that is kept at constant partial pressure for this experiment) were to be unaffected, all the lines for different polarizations should converge at the point of saturation of the benzene adsorption isotherm. This is not the case here, since the saturation rate also shifts up as  $\Delta V_{\text{WR}} > 0$ , suggesting that the bond between hydrogen and Pt gets stronger, favoring the Langmuir-Hinshelwood surface reaction step. This argument assumes, of course, that all the Pt surface participates in the reaction and not just the part that eventually becomes covered by  $\text{Na}^+$ . However, perhaps only that portion that can be poisoned by  $\text{Na}^+$  is active, in which case the change in the saturation rate can be accommodated by a purely geometric argument. We comment further on this possibility below.

It is important to compare the rates we have measured, on a somewhat nonconventional support to unsupported Pt and Pt on other supports. We can do this, based on turnover frequencies (TOF) calculated from the rate, normalizing by the oxygen uptake. At  $\Delta V_{\text{WR}} = 300 \text{ mV}$  and  $130^\circ\text{C}$ , one calculates a  $\text{TOF} = 3 \times 10^{-4} \text{ s}^{-1}$ . This value (when corrected to  $60^\circ\text{C}$  using  $E_{\text{a}} = 7.7 \text{ kcal/mole}$  (6) becomes  $4 \times 10^{-4} \text{ s}^{-1}$ ) is quite small compared with the data reported by Vannice and Lin (6) at  $60^\circ\text{C}$  using  $\text{H}_2/\text{C}_6\text{H}_6$  ratio of 20, who reported TOF values ranging from 0.036 to  $0.658 \text{ s}^{-1}$  for different Pt powders. The fact that their activity varied by an order of magnitude among different powder samples was rationalized on the basis of rapid deactivation due to the formation of carbonaceous residues. The reproducibility of the measured activity improved when a supported catalyst was used, and the observed TOF was  $0.072 \text{ s}^{-1}$  for 0.86% Pt/SiO<sub>2</sub>.

If we base our TOF on a site density estimated from the complete poisoning of the electrocatalyst by  $\text{Na}^+$ , we obtain a  $\text{TOF} 0.002 \text{ s}^{-1}$ . While still not in good agreement with the Vannice and Liu (6) numbers, this might be considered acceptable if it could be rationalized. What kind of poison could inhibit benzene hydrogenation but not chemisorption and reaction of oxygen? A wide energy XPS scan indicates almost exclusively the elements of composition with

the most intense peaks being Pt, Na and O, but there are traces of C and Li (5). The C should have been removed by a pretreatment consisting of several cycles of oxidation/reduction at 200°C in pure O<sub>2</sub> and H<sub>2</sub> before each run and the Li masked by the much more abundant Na. This question adds an element of uncertainty with regard to the interpretation of the Na<sup>+</sup> as a simple site blocker versus an inhibitor that influences the kinetics, i.e., has an electronic contribution. However, the change in slope with applied potential of the rate versus partial pressure plot (Fig. 3) suggests an electronic perturbation independent of the actual portion of the surface available for reaction.

### CONCLUSION

The results, briefly presented here, would indicate an electrophobic character (3) for the benzene hydrogenation over Pt, with Na acting as a poison for this reaction. The catalytic (chemisorptive) properties of Pt catalysts supported on β''-Al<sub>2</sub>O<sub>3</sub> can be affected significantly and reversibly by polarizing the metal–solid electrolyte interface by an externally imposed bias and thus by supplying or removing ions to or from the catalyst surface. This effect has been proposed (2–5) to lead to an electrochemically controlled spillover of ions (charge carriers) from (to) the electrolyte to (from) the metal catalyst. These ions from spillover dipoles that, due to electrostatic repulsion, spread over the whole catalyst surface forming an effective double layer (4). This electrochemical gas–metal double layer is responsible for altering the surface work function of the catalyst, perturbing in this way the chemisorptive properties of the metal.

We have proposed electronic effects to justify the poisoning character of the sodium for the benzene hydro-

genation. The possibility of some blocking (geometrical) effects or the combined effect of both factors remains. Certainly a large portion of the surface appears to be blocked for benzene hydrogenation but not for oxygen adsorption and the nature of the surface species has not been determined.

### ACKNOWLEDGMENTS

This work was supported by NSF. We thank Professor Costas G. Vayenas for very helpful discussions during the course of this research.

### REFERENCES

1. Pritchard, J., *Nature (London)* **343**, 592 (1990).
2. Vayenas, C. G., Bebelis, S., and Ladas, S., *Nature (London)* **343** (6259), 625 (1990).
3. Vayenas, C. G., Bebelis, S., Yentekakis, I. V., and Lintz, H. G., in "Catalysis Today," Vol. 11, No. 3, p. 303, Elsevier, Amsterdam, 1992.
4. Cavalca, C. A., Larsen, G., Vayenas, C. G., and Haller, G. L., *J. Phys. Chem.* **97**, 6115 (1993).
5. Cavalca, C. A., Ph.D. thesis, Yale University, 1995.
6. Vannice, M. A., and Lin, S. D., *J. Catal.* **143**, 539 (1993).
7. Yentekakis, I. V., Moggridge, G., Vayenas, C. G., and Lambert, R. M., *J. Catal.* **146**, 292–305 (1994).
8. Vayenas, C. G., Bebelis, S., and Despotopoulou, M., *J. Catal.* **128**, 415 (1991).
9. Harkness, J. R., and Lambert, R. M., *J. Catal.* **152**, 211 (1995).
10. Ratnasamy, P., *J. Catal.* **31**, 466 (1973).
11. Maslyanskii, G. N., Zharkov, B., and Rubinov, A. Z., *Kinet Katal.* **12**, 784 (1971).
12. Vannice, M. A., and Lin, S. D., *J. Catal.* **143**, 563 (1993).
13. Vayenas, C. G., Milan, M. J., Bebelis, S. I., and Neophytides, S. G., in "The Electrochemical Activation of Catalytic Reactions," Modern Aspects of Electrochemistry, Vol. 29 (J. O'M. Bockris *et al.*, Eds.), Plenum, New York, 1996.
14. Prentice, G., "Electrochemical Engineering Principles." Prentice-Hall, Englewood Cliffs, NJ, 1991.